Fracturing and calcite cementation controlling fluid flow in the shallow-water carbonates of the Jandaíra Formation, Brazil

de Graaf, Stefan; Reijmer, John J G; Bertotti, Giovanni V.; Bezerra, Francisco H R; Cazarin, Caroline L.; Bisdom, Kevin; Vonhof, Hubert B.

DOI
10.1016/j.marpetgeo.2016.12.014

Publication date
2017

Document Version
Final published version

Published in
Marine and Petroleum Geology

Marine and Petroleum Geology 80 (2017) 382–393

Contents lists available at ScienceDirect

Marine and Petroleum Geology

journal homepage: www.elsevier.com/locate/marpetgeo

Research paper

Fracturing and calcite cementation controlling fluid flow in the shallow-water carbonates of the Jandaíra Formation, Brazil

Stefan de Graaf [a, *], John J.G. Reijmer [a, f], Giovanni V. Bertotti [b, f], Francisco H.R. Bezerra [c], Caroline L. Cazarin [d], Kevin Bisdom [b], Hubert B. Vonhof [e]

[a] Faculty of Earth and Life Sciences, Sedimentology and Marine Geology Group, VU University Amsterdam, De Boelelaan 1085, Amsterdam 1081HV, The Netherlands
[b] Department of Geoscience and Engineering, Delft University of Technology, Stevinweg 1, Delft 2628CD, The Netherlands
[c] Departamento de Geologia, CCET, Federal University of Rio Grande do Norte, Natal, RN, 59078-970, Brazil
[d] Petrobras Research and Development Center, CENPES, Av Horácio de Macedo 950, Cidade Universitária, Rio de Janeiro, Brazil
[e] Max Planck Institute of Chemistry, Hahn-Meitnerweg 1, 55218 Mainz, Germany
[f] King Fahd University of Petroleum and Minerals, College of Petroleum Engineering and Geosciences, Dhahran 31261, Saudi Arabia

ARTICLE INFO

Article history:
Received 15 June 2016
Received in revised form
12 December 2016
Accepted 17 December 2016
Available online 21 December 2016

Keywords:
Geochemistry
Fluid inclusion isotope analysis
Fracturing
Calcite cementation
Fluid flow
Permeability
Jandaíra formation
Potiguar basin

ABSTRACT

The shallow-marine carbonate rocks of the Jandaíra Formation have been subject to significant permeability variations through time due to various events of fracturing and calcite cementation. As a consequence, the Jandaíra Formation accommodated fluid flow only during specific moments in time. We reconstructed these episodes of fluid flow based on isotope characterizations and microscope characteristics of calcite veins and host rock cements. The Jandaíra Formation, which belongs to the post-rift sequence of the Potiguar Basin in northeast Brazil, was deposited from the Turonian onward until a marine regression exposed it in the Campanian. Due to the subaerial exposure, meteoric waters flushed out marine connate waters, leading to an event of early diagenesis and full cementation of the Jandaíra Formation. Fluid flow through the resulting impermeable carbonate formation appears to be closely related to fracturing. Fracturing in the Late Cretaceous induced a drastic increase in permeability, giving rise to extensive fluid circulation. Host rock dissolution associated to the circulating fluids led to calcite vein cementation within the fracture network, causing it to regain an impermeable and sealing character. In the research area, fluid flow occurred during early burial of the Jandaíra Formation at estimated depths of 400–900 m. This study documents the first application of fluid inclusion isotope analysis on vein precipitates, which allowed full isotopic characterization of the paleo-fluids responsible for calcite vein cementation. The fluid inclusion isotope data indicate that upwelling of groundwater from the underlying Açu sandstones provided the fluids to the fracture network. In Miocene times, renewed tectonic compression of a lower intensity created a secondary fracture network in the Jandaíra Formation. The density of this fracture network, however, was too low to induce a new episode of fluid circulation. As a result, this tectonic event is associated with the development of barren extensional fractures.

1. Introduction

Fracturing of rocks is characteristically associated with an increase in permeability, and previously impermeable rocks may allow pervasive fluid circulation. Fracture-controlled fluid circulation has been observed in many places, and in a large range of rock types, from metamorphic bodies (e.g., Everett et al., 1999; McCaig and Wickham, 1990) to sedimentary successions (e.g., Huntoon and Lundy, 1979; Lattman and Parizek, 1964). In limestones, this fluid flow may induce dissolution and precipitation within the fracture network, eventually leading to vein cementation (e.g., Barker et al., 2006; Dietrich et al., 1983).

We address here the issue of fracturing and flow in the carbonate rocks of the Jandaíra Formation (Fig. 1) by combining structural geological observations with an isotope study of calcite

* Corresponding author.
E-mail addresses: stefan_de_graaf@hotmail.com (S. de Graaf), j.j.g.reijmer@vu.nl (J.J.G. Reijmer), g.bertotti@tudelft.nl (G.V. Bertotti), bezerrafh@geologia.ufrn.br (F.H.R. Bezerra), cazarin@petrobras.com.br (C.L. Cazarin), k.bisdom@tudelft.nl (K. Bisdom), hubert.vonhof@mpic.de (H.B. Vonhof).

http://dx.doi.org/10.1016/j.marpetgeo.2016.12.014
0264-8172/

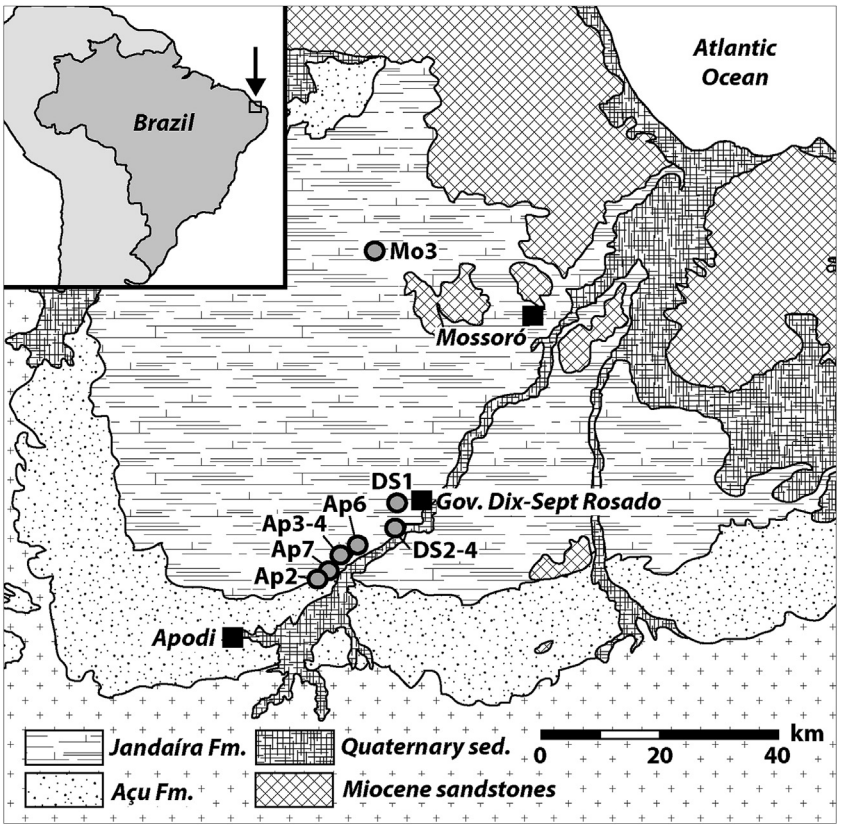

Fig. 1. Geological map of the onshore part of the Potiguar Basin (source: Serviço Geológico do Brasil) displaying the outcrop locations of the Jandaíra Formation from which vein samples were retrieved. The sandstones of the Açu Formation form a band along the southern and western edge of the Jandaíra carbonate platform due to a slight inclination (2°) of the sedimentary successions towards the northeast.

veins. The Jandaíra Formation is a Turonian-Campanian succession of shallow-water carbonates deposited during the post-rift stage of the Potiguar Basin (Sampaio and Schaller, 1968), which is one of the extensional structures in northeast Brazil related to the opening of the South Atlantic (Matos, 1992). The carbonates of the Jandaíra Formation are an excellent case study to analyse fracturing-related permeability changes because of the absence of large-scale deformation structures such as folds and faults. Compressional tectonics in this area led to the development of a dense system of fractures, veins and stylolites (Bezerra and Vita-Finzi, 2000). These structures are encountered in numerous outcropping pavements spread over a large area of ca. 2000 km^2, which allows addressing regional patterns rather than local phenomena only.

A state-of-the-art technique for fluid inclusion isotope analysis (Vonhof et al., 2006) was employed to isotopically characterize fluid inclusion water of calcite veins for both $\delta^{18}O$ and $\delta^{2}H$. As the fluid inclusions are assumed to contain the remnants of the fluid from which the veins precipitated, we were able to constrain fluid provenance and absolute precipitation temperatures of these calcite veins.

Previous studies that analysed calcite veins for fluid flow reconstruction in basins typically combine $\delta^{18}O$ values of calcite samples with homogenization temperatures of fluid inclusions to constrain $\delta^{18}O$ values of the fluid responsible for vein precipitation (e.g., Morad et al., 2010; Slobodník et al., 2006; Suchy et al., 2000; Tillman and Barnes, 1983; Zheng and Hoefs, 1993). The assumption of isotope equilibrium on which these studies rely, though, is not relevant for our methodology as it allows direct measurement of $\delta^{18}O$ values of the fluid. Furthermore, obtaining $\delta^{2}H$ values of fluid inclusions is unprecedented in this kind of study and provides a complete isotope characterization of the fluid inclusion water.

The entire set of isotope data enabled reconstruction of the fluid flow responsible for vein precipitation, including both the timing and the process of fluid supply to the fracture network. This allowed us to precisely infer how the opening of a distributed fracture system imposed major changes on the flow regime in the Jandaíra Formation.

2. The Potiguar Basin

2.1. Regional evolution

The Potiguar Basin is one of the Brazilian marginal basins that formed as a result of the rifting of Gondwana, which separated the continents of Africa and South America (Matos, 2000; Ojeda, 1982). Breakup of the continental crust of Gondwana was accomplished in the Early Cretaceous (Matos, 1992). Proterozoic NE-SW and E-W trending shear zones, which were formed in the basement rock during the Brasiliano/Pan-African orogeny, were reactivated as normal faults controlling the formation of three NE-SW trending intracontinental rift basins in northeast Brazil; the Potiguar Basin is one of these (Brito Neves et al., 1984; De Castro et al., 2012). The rift basins are characterized by NW-SE oriented transfer faults and basement highs separating various asymmetric half-grabens (Matos, 1999).

Rifting and normal faulting in the Potiguar Basin began in the Berriasian and ceased in the Barremian (Chang et al., 1992; Matos, 1992). The post-rift stage is characterized by subsidence increasing towards the offshore region in the NE, allowing for the deposition of post-rift sedimentary successions thickening towards the NE

(Matos, 2000).

Apatite fission track data suggest the existence of various events of uplift in northeast Brazil after deposition of the Jandaíra Formation, with a main event in the Middle to Late Cenozoic (Da Nóbrega et al., 2005; Morais Neto et al., 2009). The uplift is documented throughout the integrity of northeast Brazil, including the marine carbonates in the Paraíba area (Barbosa et al., 2003), the Recôncavo-Tucano-Jatobá Rift (Japsen et al., 2012), the São Francisco Craton (Harman et al., 1998) and the Borborema Province (Almeida et al., 2015; Luz et al., 2015). The exact cause of the Middle to Late Cenozoic uplift remains subject to debate. Morais Neto et al. (2009) suggest climate change as an instigator for increased erosion and uplift. Other explanations rely on compressional stresses induced by the Andean orogeny (Peulvast et al., 2008), or igneous activity like deep-seated mantle plumes (Mizusaki et al., 2002) and magmatic underplating (Oliveira and Medeiros, 2012).

2.2. The Açu and Jandaíra Formations

The Açu and Jandaíra Formations, both part of the post-rift sedimentary succession, are the two units relevant to our study. In the onshore part of the Potiguar Basin, these units display a combined thickness of 200–700 m (De Castro, 2011). The Açu Formation was deposited in the onshore part of the Potiguar Basin during the Albian and Cenomanian (Araripe and Feijó, 1994). It comprises fluvial-estuarine sandstones and mudstones, which represent a period of non-marine sedimentation in the Potiguar Basin at the onset of the post-rift stage. Deposition of the Açu sandstones retreated progressively landward because of subsidence-induced transgression until marine conditions dominated over the entire Potiguar Basin in the Turonian (Ojeda, 1982). This transgression led to the deposition of the Jandaíra carbonate platform from the Turonian to the Campanian (Sampaio and Schaller, 1968).

The Jandaíra limestones encountered in the study area are principally mudstones, peloidal packstones and grainstones. Differential degrees of dolomitization indicate that desiccation played an important role during deposition. Sedimentation in a lagoonal environment was inferred from the sheer amount of pellets and the fossil content, consisting of bivalves, molluscs and green and red algae. Shallow marine depositional environments for the Jandaíra Formation were also deduced from ostracode assemblages (Delicio et al., 2000; Santos Filho et al., 2015).

At present, the sedimentary succession of the Potiguar Basin displays a minor and regular bedding dip of ~2° towards the NE (Maia and Bezerra, 2015). As a result, the Açu Formation crops out in a band of 10–20 km wide to the south and west of the Jandaíra carbonate platform (Fig. 1).

3. Fractures, veins and stylolites in the Jandaíra Formation

3.1. The database

The database gathered during the study consists of isotope data and structural geological observations of 17 outcrops mainly from the southern stretches of the onshore Potiguar Basin (Fig. 1). The structures observed in the Jandaíra Formation include large-scale open fractures and smaller-scale fractures, veins and stylolites. The focus of this publication is on the implications of petrographic and isotope studies of vein samples. A portable diamond core drill was operated to retrieve a total of 31 oriented vein samples from key localities (Table 1). These veins samples were subject to stable carbon and oxygen isotope analysis and, if containing a vein sufficiently wide (>4 mm), to fluid inclusion isotope analysis.

Table 1
Provenance of the cored vein samples following the UTM system.

Outcrop	Coordinates (UTM)	Cored vein samples
Ap2	24M 0648176, 9385026	Ham1, Ham2, Ham5
Ap3	24M 0650636 9387810	Ham15, Ham18, Ham21
Ap4	24M 0652108 9388522	Ham9, Ham10
Ap6	24M 0653790 9390149	JD6, JD7, JD8, JD9, JD10, JD11
Ap7	24M 0649030 9384916	JD13, JD14, JD15
DS1	24M 0660353 9396140	JD1, JD2
DS2	24M 0659906 9392295	JD3, JD4, JD5
DS3	24M 0660737 9392361	JD19, JD20, JD21
DS4	24M 0660645 9392270	JD22, JD23, JD24
Mo3	24M 0653815 9390089	JD16, JD17, JD18

3.2. Structures

An approximate total of 300 measurements of the small-scale deformation structures were made across all researched outcrops of the Jandaíra Formation. The observed fractures and stylolites display a high degree of consistency in type and arrangement over the entire research area (Bertotti et al., 2016).

The dominant features observed in the outcrops of the Jandaíra Formation are small-scale sub-vertical fractures with a generally consistent N-S to NNE-SSW strike. These fractures characteristically occur as veins containing a calcite infill of up to 1 mm wide. On a larger scale, a network of open fractures with a typical aperture of 5–50 cm occurs. About 10.000 of these open fractures were manually traced from aerial images acquired by Bertotti et al. (2016). The open fractures display similar orientations to the small-scale sub-vertical fractures. For this reason, the latter probably formed weak zones in the rock, which opened during the Middle to Late Cenozoic exhumation. The thus created open fractures further widened in association with widespread epigenetic karstification due to infiltration of surface waters (Fernandes et al., 2015).

Sub-vertical stylolites are common throughout the research area and are oriented E-W to NW-SE. These stylolites are perpendicular to the N-S to NNE-SSW striking sub-vertical fractures, which are, therefore, interpreted to be co-genetic. The co-genetic relationship of these structures is also demonstrated by occurrences of sub-vertical fractures passing into sub-vertical stylolites. The sub-vertical fractures and sub-vertical stylolites are interpreted to result from NNE-SSW trending tectonic compression. This particular stress-field has previously not been studied extensively leaving its exact causes and timing to be unknown. The systematic orientation of the sub-vertical fractures and their association with the sub-vertical stylolites does seem to indicate that the stress-field was caused by plate wide tectonic stresses, which are commonly observed in passive margins due to ridge push and gravitational forces resulting from lateral variations in lithosphere structure across the margin (Pascal and Cloetingh, 2009).

A second set of stylolites is bedding-parallel and is, therefore, interpreted as having formed during burial. As these sub-horizontal stylolites overprint the sub-vertical veins (Fig. 2), we conclude that the sub-vertical structures formed during post-rift subsidence following full lithification and cementation of the carbonates. Therefore, the timing of the NNE-SSW stress-field should be placed in Late Cretaceous to Early Tertiary times.

A second compressional stress-field affecting the Jandaíra Formation acted from the Miocene onwards (Lima et al., 1997; Reis et al., 2013). The Miocene compression is oriented parallel to the coast, and is attributed to the interplay of far-field tectonic stresses and coast-perpendicular tensional stresses caused by a difference in density between the continental and oceanic crust in northeast Brazil (Assumpção, 1992; Ferreira et al., 1998). The Miocene stress

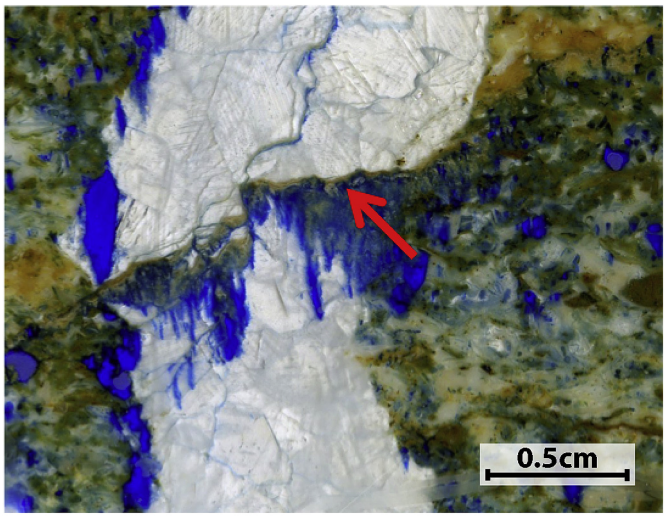

Fig. 2. A scan of the vertically-oriented thin section of sample JD4. The cross-cutting relation of the sub-vertical vein and a sub-horizontal stylolite indicates that fracturing and vein infill predated burial stylolite formation. Blue colouring is due to blue epoxy resin filling open pore space in the samples. (For interpretation of the references to colour in this figure legend, the reader is referred to the web version of this article.)

field induced a second phase of minor fracturing and stylolite formation in the Jandaíra Formation. The focus of this study, though, was on the Late Cretaceous structures as the fractures related to the Miocene phase of compression lack vein infill in contrast to those of Cretaceous age.

3.3. Veins

3.3.1. Field and macroscopic observations

Fractures related to the NNE-SSW compressional event are commonly cemented by a calcite infill. These veins typically exhibit opening purely perpendicular to the fracture plane. Additionally, a substantial amount of the veins display characteristics of strike-slip shear as identified from releasing/constraining bends and en-echelon structures. Fractures that display both an extensional as a shear component are commonly referred to as hybrid fractures and display dihedral angles lower than shear fractures (Hancock, 1985). The dihedral angle displayed by the conjugate hybrid fractures related to NNE-SSW compression centres around 20°. The sub-vertical position of the conjugate sets indicates fracturing under a vertical position of the intermediate stress. This implies formation under a different stress regime than the burial stylolites, which require the principal stress to be vertical.

The calcite veins reach thicknesses of up to 12 mm and exhibit lengths of up to several metres. Thin veins (<2 mm wide) display sharp and generally matching walls. Matching walls in this context are veins walls that would seal perfectly in case the calcite infill were to be removed. This is the case if vein walls experienced no further modifications after initial fracturing. Walls of thicker veins on the contrary are more irregular and non-matching as a result of dissolution along the fracture planes prior to calcite precipitation. The associated increase in concentration of dissolved $CaCO_3$ possibly facilitated calcite precipitation and cementation of the fractures (e.g., Buhmann and Dreybrodt, 1985; Reddy et al., 1981).

3.3.2. Microscope observations

Thin sections were manufactured to study the calcite infill and identify abutment relations between veins and horizontal stylolites. The fractures are in general homogeneously filled in with blocky calcite crystals that can get as large as 10 mm. Veins cut through the entire rock inclusive of sparite cement filling primary porosity (Fig. 3a), suggesting that fracturing took place following cementation of the pore-filling sparites. The brighter appearance of the fracture infill compared to the pore-filling sparite cements illustrates the different nature of these cements.

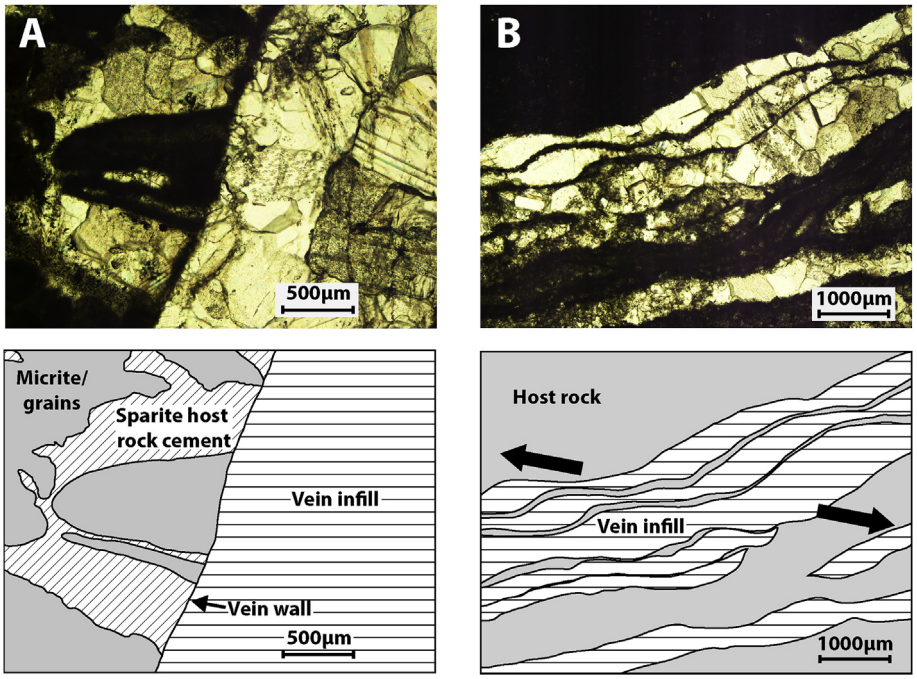

Fig. 3. Detailed large magnification pictures of the thin sections show that (a) the vein walls are sharp and form a distinct boundary also on places where the vein borders pore-filling sparite cements in the host rock. These cements belong, thus, to a different stage of calcite precipitation than the vein infill. Multiple bands of infill are commonly present (b), indicating multiple stages of opening and infill. The constraining bends visible in the bands of infill demonstrate the presence of a strike-slip shear component during fracture opening.

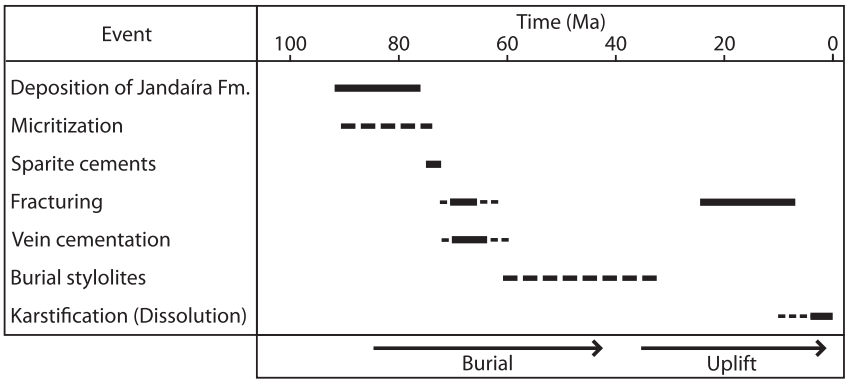

Fig. 4. The paragenetic sequence of the Jandaíra Formation displays two events of fracturing. Vein infill is associated only to fractures dating to the Late Cretaceous. Sparite cements filling up pore space in the Jandaíra limestones represent an earlier event of calcite precipitation during early burial diagenesis. Initiation of uplift is poorly constrained and is given here solely as an indication.

Abutment relations between veins and sub-horizontal burial stylolites suggest that fracture infill occurred during early burial since the burial stylolites cut through the calcite vein infill (Fig. 2). Multiple generations of vein infill were recognized in veins thicker than 2 mm marked by the occurrence of bands of calcite infill separated by thin darker domains (Fig. 3b), which possibly formed due to repeated opening and infill following a crack-and-seal mechanism (Ramsay, 1980). This would imply that fractures were filled in contemporaneously with fracture opening during the early burial stage of the Jandaíra Formation.

3.4. Paragenetic sequence

The field and microscope observations allow constructing a paragenetic sequence for the Jandaíra Formation (Fig. 4). The first paragenetic phase after deposition and micritization is represented by sparite cements filling in pore space in the host rock. Subsequently, a phase of wholesale fracturing of the Jandaíra Formation is recognized during early burial in Late Cretaceous to Early Tertiary times. The paragenetic sequence includes one event of vein cementation, which took place concurrent with fracturing in the Late Cretaceous to Early Tertiary. Vein cementation was followed up by the formation of horizontal burial stylolites as the Jandaíra Formation continued to subside. Renewed tectonic compression in Miocene times is characterized by the development of barren fractures. Secondary porosity is commonly visible in the Jandaíra limestones. This porosity is identified to have formed latest and is most likely related to the recent period of karstification.

4. Isotope data

4.1. Methodology

4.1.1. Stable isotope analysis of calcite material

The thin sections were sampled with a Merchantek Micromill for carbon and oxygen isotope analysis of the calcite vein infill, the host rock micrites and the pore-filling sparite cements in the host rock. The majority of the vein samples were drilled in high-resolution transects across the veins (Fig. 5) to detect possible isotope variation within the infilling stages of the veins.

Samples were analysed on a Thermo Finnigan Delta + mass spectrometer equipped with a GASBENCH II preparation device. Around 10 μg of $CaCO_3$ sample, placed in a He-filled 3 ml exetainer vial was digested in concentrated anhydrous H_3PO_4 at a temperature of 45 °C. Subsequently, the CO_2-He gas mixture was transported to the GASBENCH II in a He carrier flow. In the GASBENCH, water was extracted from the gas through nafion tubing, and CO_2 is analysed in the mass spectrometer after separation of other gases in a GC column. Isotope values are reported as $\delta^{13}C_C$ and $\delta^{18}O_C$ ratios relative to VPDB. The reproducibility (1σ) of routinely analysed lab calcite standards is better than 0.1‰ for $\delta^{13}C_C$ and 0.15‰ for $\delta^{18}O_C$.

4.1.2. Fluid inclusion isotope analysis

Water from fluid inclusions in the calcite veins was analysed for δ^2H_W and $\delta^{18}O_W$ by applying the methodology developed by Vonhof et al. (2006, 2007). This technique allows for isotope characterization of fluid inclusion water of calcite vein samples of 0.4–2 g. The samples were crushed in the Amsterdam device, which is a crusher unit connected to a continuous-flow pyrolysis furnace (ThermoFinnigan TC-EA). The sub-microliter amount of water that is released due to the opening of inclusions is vaporised and transported to a TC-EA reactor tube, which separates the water vapour in H_2 and CO gas as a result of reaction with glassy carbon at 1400 °C. A cryo-focusing technique is applied prior to entry into the reactor tube to generate a water pulse short enough to be analysed. The H_2 gas and CO gas are separately measured in a continuous-flow isotope-ratio mass spectrometre (ThermoFinnigan Delta XP). A rapid magnet peak jump between the entries of H_2 gas and CO gas allows analysis of both hydrogen and oxygen isotopes from a single

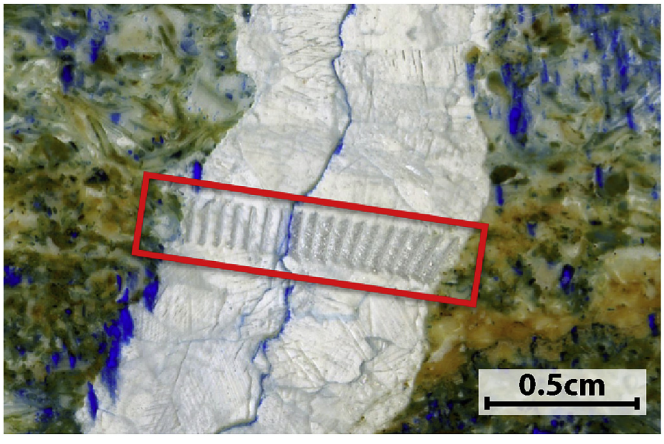

Fig. 5. A scan of a thin section of sample JD4 showing the locations of multiple closely-spaced calcite samples micromilled across a calcite vein. A clear suture is visible in the middle of the vein, showing the progressive inward growth of the calcite vein infill. Blue colouring is due to blue epoxy resin filling open pore space in the samples. (For interpretation of the references to colour in this figure legend, the reader is referred to the web version of this article.)

water release. Isotope values are reported as δ^2H_W and $\delta^{18}O_W$ ratios relative to the VSMOW standard. Routinely measured water standards following this analytical protocol were reproducible (1σ) within 0.23‰ for $\delta^{18}O_W$ and 1.30‰ for δ^2H_W.

5. Results

5.1. Stable isotope analysis of calcite material

We have performed carbon and oxygen stable isotope measurements on 284 samples retrieved from the thin sections. Most of them are organised in transects across the veins. Additionally, we have executed measurements on host rock micrites and on sparites forming the intragranular cement in coarser parts of the Jandaíra carbonates.

In a cumulative graph of all measurements, data are clustered in three different domains (Fig. 6). Host rock micrites display $\delta^{13}C_C$ values varying from −2.70 to 1.95‰. Highly variable isotope values are recorded for oxygen isotopes with $\delta^{18}O_C$ values ranging from −11.47 to −0.62‰. A statistically significant positive correlation exists between $\delta^{18}O_C$ and $\delta^{13}C_C$ in the host rock micrites.

Porosity-filling sparite cements in the host rock record $\delta^{13}C_C$ values similar to the host rock micrites (−1.42–2.30‰). $\delta^{18}O_C$ values of these sparite cements (−11.45 to −8.91‰) are remarkably consistent and coincide with the lowest $\delta^{18}O_C$ values recorded in the host rock micrites.

The isotope composition of the veins defines a field significantly different from that of the micrites and pore-filling sparites in the host rock. $\delta^{18}O_C$ values plot in a narrow range between −10.95 and −7.19‰, which is slightly higher than those of the pore-filling sparite cements in the host rock. The vein transects show little internal variation in $\delta^{18}O_C$ (Fig. 7). Furthermore, notable differences are absent between veins from the various outcrops throughout the entire research area.

Carbon isotope values of the veins show a larger variability, from −6.49 to 2.17‰, thus covering a wide range that stretches to significantly lower values compared to the micrites and pore-filling sparites in the host rock. Variation within transects are significantly higher for $\delta^{13}C_C$ values compared to the $\delta^{18}O_C$ values of the same samples (Fig. 7).

5.2. Fluid inclusion isotope analysis

The fluid inclusion water of ten vein samples was analysed for δ^2H_W and $\delta^{18}O_W$ (Table 2). Fluid inclusion isotope analysis was only performed on samples from outcrops in the southwestern part of the Potiguar Basin, as veins from the Mossoró outcrops were not suitable for extraction of a sufficient amount of vein material. The isotope data obtained from fluid inclusion isotope analysis are taken to reflect the isotope signature of the fluid from which the veins precipitated. The data are plotted in Fig. 8 along with the Global Meteoric Water Line (GMWL), which expresses the relation between δ^2H_W and $\delta^{18}O_W$ in meteoric waters as a global average (Craig, 1961). The data plot reasonably close to the GMWL, suggesting a meteoric origin of the fluid that produced the vein calcites.

5.3. Vein cementation temperatures

Oxygen isotope fractionation between water and calcite is, under the assumption of isotope equilibrium conditions, uniquely dependent on temperature (O'Neil et al., 1969). Therefore, calcite precipitation temperatures can be constrained for vein samples of which both the calcite and fluid inclusion water were analysed for oxygen isotopes. The combination of $\delta^{18}O$ values yields oxygen isotope fractionation factors during vein precipitation. The temperature equation provided by Kim and O'Neil (1997) was employed to calculate calcite precipitation temperatures from these fractionation factors. Calculated temperatures for the samples range from 36 to 48 °C (Table 2).

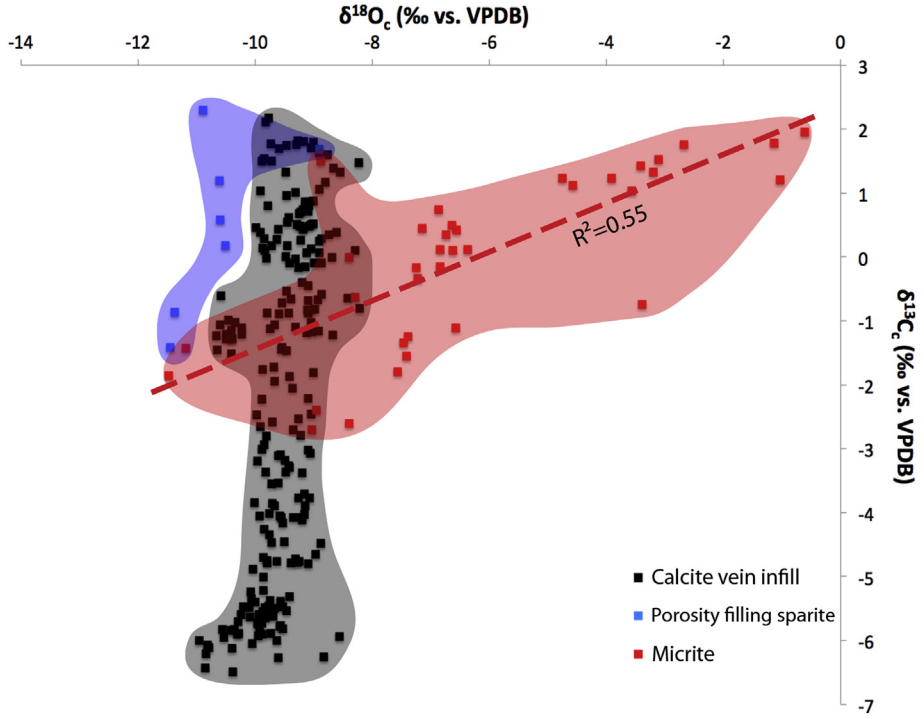

Fig. 6. The stable isotope measurements display a narrow range of $\delta^{18}O_C$ values for the calcite vein infill and pore-filling sparite cements. Compared to the host rock, the vein calcites display more negative $\delta^{13}C_C$ values. The host rock micrites display a positive relation between $\delta^{13}C_C$ and $\delta^{18}O_C$.

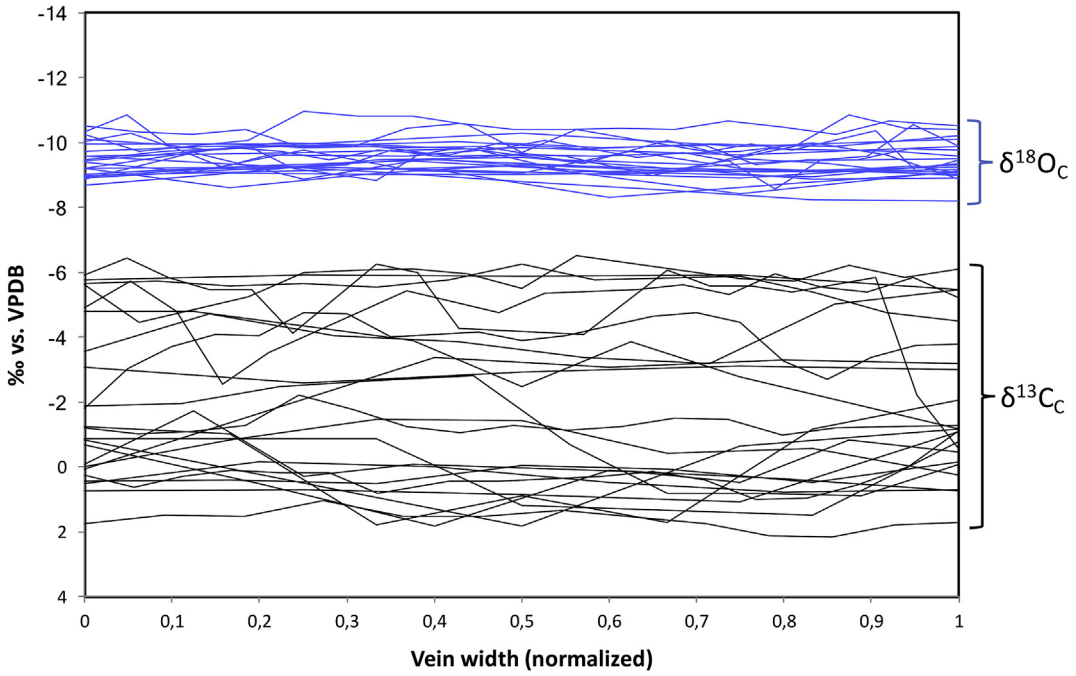

Fig. 7. Composite plot of the vein transects from the stable isotope analysis with normalised vein widths. Oxygen isotope values (blue) occupy a narrow range across the transects in contrast to carbon isotope values (black), which display a significantly higher degree of variation both between veins as within individual veins. (For interpretation of the references to colour in this figure legend, the reader is referred to the web version of this article.)

5.4. Implications of the isotope data

5.4.1. Early diagenesis by meteoric waters

The isotope values of the diagenetic calcites exhibit distinct ranges of $\delta^{18}O_C$ and $\delta^{13}C_C$ values (Fig. 6). The micrites are the first paragenetic phase recognized and range from relatively high $\delta^{13}C_C$ and $\delta^{18}O_C$ values that fit early diagenesis in the marine realm (Hoefs, 1973; Hudson, 1977) towards lower $\delta^{13}C_C$ and $\delta^{18}O_C$ values that likely resulted from progressive diagenetic alteration in meteoric or burial conditions. The next paragenetic phase is represented by the pore-filling sparites in the host rock, which coincide isotopically with the most depleted $\delta^{18}O_C$ values of the micrite range (−11‰). We take this to suggest that the pore-filling sparites are merely the next step in the ongoing diagenetic isotope depletion. This depletion could have resulted from either the heating of marine connate fluids during burial, or the increasing influence of isotopically depleted meteoric fluids. Assuming isotope equilibrium and a marine fluid, precipitation temperatures of the pore-filling sparites should be around 80 °C. A meteoric fluid with initially lower $\delta^{18}O$ values could precipitate sparite at much lower temperatures.

With calcite stable isotope data alone, it is not possible to discriminate between these two scenarios. The vein calcites representing the third and deepest paragenetic phase of calcite precipitation, however, supply additional information that strongly favours the meteoric fluid scenario for the paragenetic phases of the micrites and the pore-filling sparites.

Crucial information comes from the fluid inclusion isotope ratios of the vein calcites. First of all, the δ^2H_W and $\delta^{18}O_W$ values of the inclusion water indicate a meteoric fluid at depth during the stage of vein cementation, making it probable that the earlier diagenetic phases were under the influence of meteoric fluids as well. Secondly, the highest calculated precipitation temperature of the vein calcites at 48 °C makes it highly unlikely that earlier (i.e., shallower) diagenetic phases could have precipitated at temperatures around 80 °C that the scenario with marine fluids would require.

The evidence presented suggests, thus, a diagenetic scenario in which meteoric water is the dominant fluid during all the carbonate phases encountered, even though part of the diagenetic alteration occurred in the burial realm. In this scenario, meteoric

Table 2
$\delta^{18}O_W$ and δ^2H_W values obtained from the fluid inclusion isotope analysis and corresponding calcite precipitation temperatures. An error margin of 2σ was employed for temperature calculation.

Sample	Outcrop	$\delta^{18}O_W$ (±0.46‰ vs. VSMOW)	δ^2H_W (±2.60‰ vs. VSMOW)	$\delta^{18}O_C$ (‰ vs. VPDB)	Precipitation temperature (°C)
JD3	DS2	−5.3	−29.2	−9.70 ± 0.05	36.6 ± 2.7
JD4	DS2	−5.0	−17.8	−9.65 ± 0.06	38.2 ± 2.8
JD5	DS2	−4.6	−28.8	−9.56 ± 0.30	40.1 ± 4.2
JD6	Ap6	−4.0	−21.0	−9.79 ± 0.08	44.6 ± 3.1
JD8	Ap6	−3.9	−18.4	−9.39 ± 0.11	42.6 ± 3.2
JD10	Ap6	−3.6	−18.9	−9.07 ± 0.11	42.6 ± 3.2
JD15	Ap7	−3.5	−23.3	−9.92 ± 0.06	48.0 ± 3.0
JD22[a]	DS4	−5.1	−26.7		
JD23	DS4	−4.4	−16.2	−10.58 ± 0.11	46.9 ± 3.3
JD24	DS4	−4.8	−36.4	−10.37 ± 0.06	43.4 ± 2.9

[a] No reliable $\delta^{18}O_C$ value obtained, impeding precipitation temperature calculation.

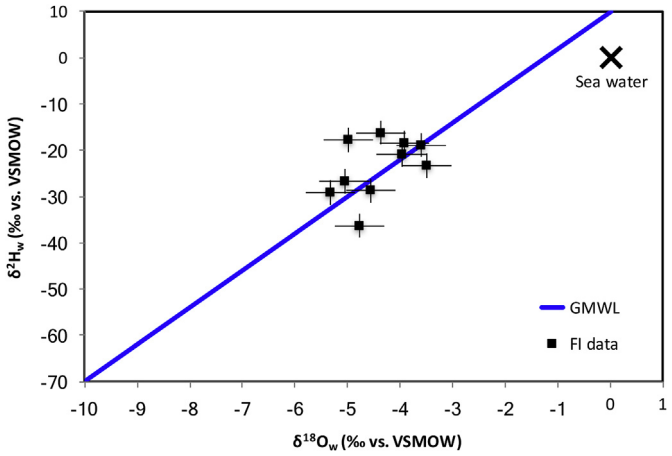

Fig. 8. The fluid inclusion water of ten vein samples was analysed for stable oxygen and hydrogen isotopes. The fluid inclusion data reveal a meteoric origin of the fluid. The isotope composition characteristic for seawater is represented by a cross in the upper right corner.

conditions prevailed already rapidly after deposition of the shallow marine limestones of the Jandaíra Formation. Marine connate fluids were probably flushed out by meteoric waters due to a marine regression, which marked the end of deposition of the Jandaíra Formation.

5.4.2. Characterization of the fluid responsible for vein cementation

The low variability in the oxygen isotope data of the vein cements indicates that a single isotopically and thermally stable fluid was responsible for vein precipitation in the Jandaíra Formation. This fluid was meteoric in origin and acted on a regional scale, as no notable oxygen isotope differences are present between veins from the various outcrops throughout the entire research area.

The similarity in $\delta^{13}C_C$ signature of the pore-filling sparite cements and the host rock micrites indicates that the carbon for the event of pore infill by sparite cements originated mainly from dissolution of the Jandaíra limestones due to the direct entry of meteoric water from the surface. The wider range of $\delta^{13}C_C$ values in the subsequent vein cementation event implies that a second source of carbon with much lower $\delta^{13}C_C$ values was drained (Fig. 9). This probably resulted from fracture opening, which induced a change in fluid flow patterns. The variable carbon isotope data indicate that the two sources of carbon had a variable contribution through time and space. Exact constraints on the frequency of these variations, though, cannot be provided from the isotope data.

6. Discussion

Veins in the Jandaíra Formation form a network with geometric characteristics consistent over distances of tens of kilometres (Bertotti et al., 2016) suggesting that the flow responsible for the deposition of the vein infill was on a regional scale and driven by regional pressure differences. Faults are very scarce in the area and only few of them provide evidence of hydrothermal alteration. As a consequence, fluid motion in the Jandaíra Formation was achieved mainly by flow through the fracture network.

6.1. Timing of fluid flow

The isotope data do not provide sufficient information regarding the timing of fluid flow and subsequent vein infill in the Jandaíra carbonates. Consequently, the age of the hydrogeological system responsible for vein cementation cannot be inferred from the isotope data alone. Structural geological observations, though, can provide additional clues to still deduce the beginning and end of the flow system that led to the formation of the veins we have studied.

Crack-and-seal structures imply that veins progressively

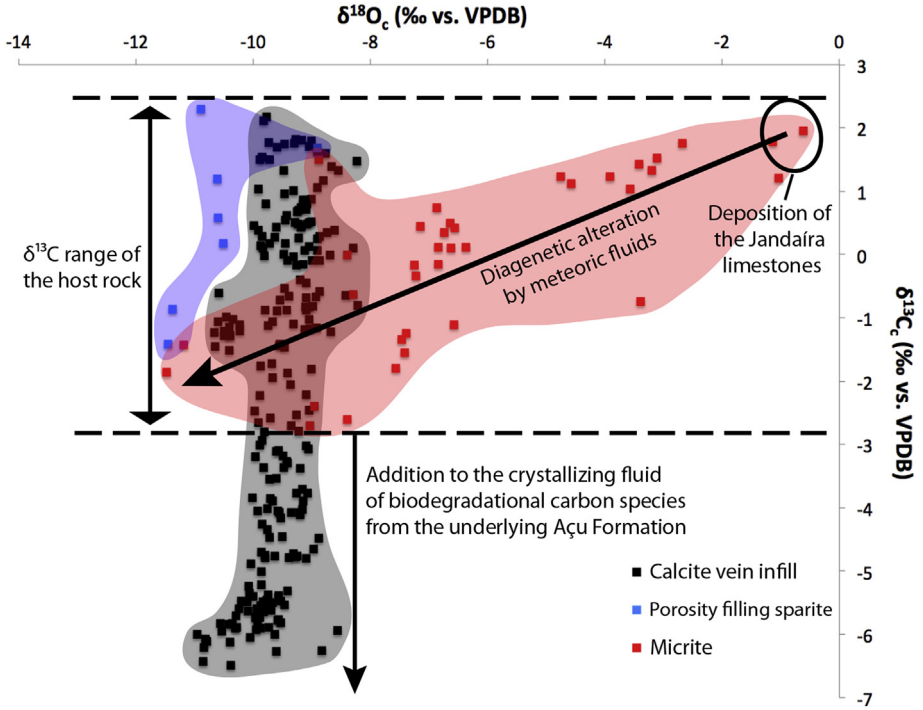

Fig. 9. The stable isotope data provide evidence for diagenetic alteration of the host rock micrites after deposition due to entry of meteoric waters. The low (<−3‰) $\delta^{13}C_C$ values recorded by the veins can best be explained by addition of remineralized organic carbon, which is possibly derived from the underlying Açu Formation.

widened due to a cyclic mechanism of repeated opening and infill. Hence, fluid flow and calcite vein formation within the Jandaíra Formation occurred at the same time as brittle fracturing in the Late Cretaceous. The sub-vertical position of the conjugate fracture sets in which the veins precipitated requires a horizontal principal stress in contrast to a vertical principal stress that is necessary for the formation of horizontal stylolites. Therefore, synchronous development of these burial stylolites and the sub-vertical veins is unconceivable. Because the sub-horizontal stylolites overprint the sub-vertical veins (Fig. 2), we conclude that fluid flow and vein cementation occurred during early burial of the Jandaíra carbonates probably in Late Cretaceous to Early Tertiary times.

Because flow in the Jandaíra Formation was not localised along faults, we assume that temperature anomalies related to fluid advection were minor and that, therefore, precipitation temperatures relate directly to precipitation depths. Turner (2008) found a paleo-geothermal gradient of 35 °C/km and a paleo-surface temperature of 20 °C for the similar Brazilian intracontinental rift basin of Sergipe-Alagoas in the Late Cretaceous. Applying these data, the precipitation temperatures of 36–48 °C indicate vein precipitation at depths of 475–800 m. The calculated precipitation temperatures can be considered realistic as apatite fission track data from the region indicate rock temperatures reaching up to 60–80 °C during maximum burial in the Middle to Late Cenozoic (Morais Neto et al., 2009).

We conclude that the episode of fracturing that activated fluid flow through the Jandaíra carbonates took place during early burial at depths of approximately 400–900 m in the Late Cretaceous to Early Tertiary (Fig. 10). It should be noted that the depth estimate is valid only for the research area as the amount of post-rift subsidence varies throughout the Potiguar Basin.

6.2. Provenance of vein-related flow

The isotope data of the Jandaíra carbonates and its calcite veins provide valuable constraints on the characteristics of the fluid circulating through the fracture system that eventually led to vein cementation. The first relevant observation is that the isotope composition of the fluid corresponds to that of meteoric waters (Fig. 8). These waters might have come from above in the form of direct precipitation or might have been flowing laterally from a distant recharge area.

The hypothesis of calcite precipitation associated with waters originating directly from precipitation falling in the study area is incompatible with the variations in isotope composition we document. Towards the SW, $\delta^{18}O_W$ values display a landward increase from −5.3‰ to −3.5‰ (Fig. 11). Theoretically, $\delta^{18}O_W$ values of precipitation decrease landward (Dansgaard, 1964). Therefore, the observed trend is unlikely to have been achieved through local meteoric recharge, and lateral flow of groundwater must have been indispensable in the process of supplying the fluid to the fracture network.

This lateral flow is most likely accommodated by the porous sandstones of the Açu Formation that directly underlies the Jandaíra formation. The flow of meteoric waters along the Açu confined aquifer in Late Cretaceous times is documented by the chemistry of authigenic K-feldspar overgrowths around grains of detrital orthoclase and microcline (Maraschin et al., 2004). Climate forced isotope variations of the rainwater in the recharge zone of the Açu aquifer can create isotope trends throughout the aquifer's water as observed in the present-day Açu Formation by Frischkorn and Santiago (2000). The observed trend in $\delta^{18}O$ values can then be attributed to the variable distance of the outcrops to the recharge zone. A provenance of the fluid from the Açu Formation is further supported by the close resemblance in isotope values of the fluid and the present-day groundwater in the Açu Formation, which exhibits isotope values ranging from −2.5 to −4.8‰ for $\delta^{18}O_W$ and −16 to −32‰ for $\delta^{2}H_W$ (Frischkorn et al., 1988).

The second relevant observation is that oxygen isotope values of the calcite veins are homogeneous throughout the study area, suggesting precipitation from a single fluid flowing in a distributed manner through the entire Jandaíra Formation. Carbon isotope ratios, on the other hand, vary in a non-systematic manner and point to the existence of two sources of carbon for calcite precipitation. The upper boundaries of $\delta^{13}C_C$ values of the vein material and of the host rock coincide at approximately 2‰, indicating that the supply of carbon from host rock dissolution was the primary source of carbon. Pressure solution along stylolitic surfaces contributed greatly to the process of dissolving the host rock. The presence of ubiquitous host rock dissolution also became apparent from the non-matching character of the vein walls.

The secondary source must have had highly negative $\delta^{13}C_C$ values, and is therefore likely represented by methane and CO_2 released from the degradation of organic matter. Methane, which is typically produced by bacterial degradation at shallow burial conditions (<100 °C), would be highly depleted in ^{13}C exhibiting $\delta^{13}C_{VPDB}$ values down to −80‰ (Stahl, 1979). Produced CO_2 would be slightly less depleted averaging at a $\delta^{13}C_{VPDBB}$ value of −24‰ (Hudson, 1977). Addition of these ^{13}C-depleted types of carbon to a

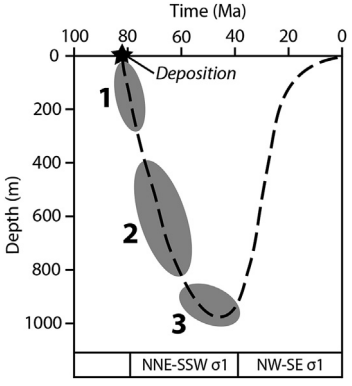

Fig. 10. Schematic representation of the vertical movements experienced by the Jandaíra Formation through time in the region of Apodi and Dix-Sept, showing early diagenesis by a meteoric fluid (1), fracturing and fluid flow (2) and horizontal stylolite formation (3). Exact depths may vary throughout the Potiguar Basin due to variable subsidence. The exact ages of the events are subject to uncertainty.

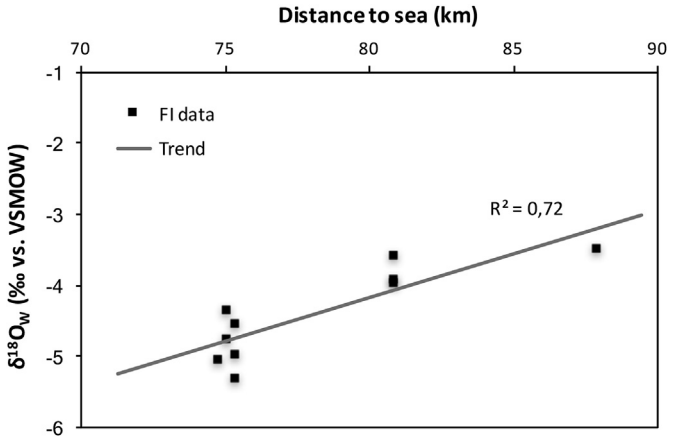

Fig. 11. The relation between $\delta^{18}O_W$ values from the fluid inclusion isotope analysis and the distance to sea of the samples shows a landward increase in $\delta^{18}O_W$.

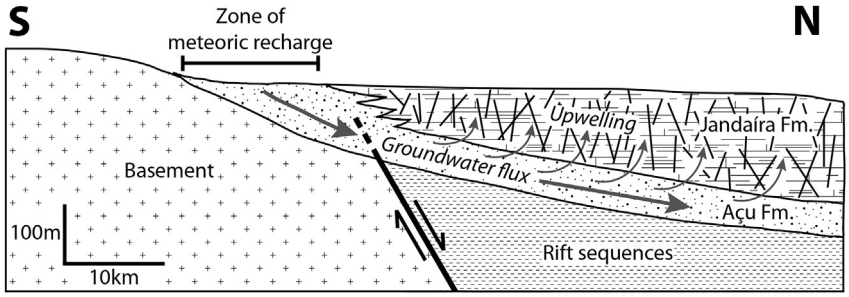

Fig. 12. The hydrogeological setting during vein cementation in the Late Cretaceous. The fully cemented Jandaíra formation functioned as a seal prior to fracturing and an undisturbed northeast-ward groundwater flux was present within the confined aquifer of Açu sandstones. Fracturing caused an increase in the permeability of the Jandaíra Formation, and pervasive fluid circulation initiated by means of upwelling of groundwater from the underlying Açu Formation.

carbonate-rich fluid can bring down $\delta^{13}C_C$ values of calcite precipitates significantly (e.g., Prikryl et al., 1988; McManus and Hanor, 1988).

The carbon species were most likely derived from hydrocarbons and other organic constituents in the underlying Açu Formation. Fracturing managed to establish pathways towards the Açu Formation, which allowed abundant carbon species to be supplied to the fracture network of the Jandaíra Formation (Fig. 9).

6.3. Late Cretaceous hydrogeology

Based on the interpretations presented above, we present a schematic representation of the setting of the Jandaíra Formation at the time of fluid flow and vein cementation (Fig. 12). Both are part of the post-rift succession of the Potiguar Basin and show a thickening/deepening trend towards the NE as a consequence of the strong thermal subsidence associated with rifting in the Equatorial Atlantic (Matos, 2000). Due to marine transgression in the post-rift stage, which caused a progressive retreat of the depositional centres of the Açu and Jandaíra Formations, we make the safe assumption that the Jandaíra carbonates passed laterally towards the SW into the fluvial system of the Açu sandstones and eventually to exposed basement and pre-to syn-rift rocks. This implies that the outcropping band of Açu sandstones to the SW was already present in Late Cretaceous times. Rainwater charged into the outcropping zone of Açu sandstones flowed towards the NE underneath the impermeable Jandaíra Formation. As already mentioned in §6.2, the flow of meteoric waters through the Açu confined aquifer in Late Cretaceous times was also documented by Maraschin et al. (2004).

Based on the arguments presented in previous sections, we estimate that the rocks we have investigated were at a depth of 400 m at the onset of fracturing. Layer-parallel shortening associated with NNE-SSW maximum compression was accommodated by the formation of sub-vertical extensional to hybrid fractures, all with a significant aperture, distributed over the entire region of the outcropping Jandaíra carbonates. The episode of fracturing had a major influence of the hydrogeology of the area as the Jandaíra Formation became a permeable body, thereby losing the sealing character it had until that moment. Pushed by the hydraulic head, water charged in the area of outcropping fluvial sandstones now flowed both along the Açu Formation and upward along the pathways formed by the fracture network in the Jandaíra Formation.

The time interval characterized by upward flow through the Jandaíra Formation lasted until calcite was precipitated in the open fractures, filling up the fluid pathways and eventually preventing further flow. Part of the dissolved carbon species necessary for calcite precipitation originated from the degradation of organic matter in the Açu sandstones. The largest part, however, was associated with the ubiquitous dissolution of host rock material as indicated by the large overlap in $\delta^{13}C_C$ values of the vein cements and the host rock (Fig. 9). The sealing of fractures by vein infill documents the end of flow through the Jandaíra Formation, which likely regained its role of impermeable seal in the hydrogeological system afterwards.

6.4. Fracture-dependency of fluid flow

Already before the onset of fracturing during early burial in the Late Cretaceous, the Jandaíra Formation had become an impermeable unit due to the infilling of intragranular pore space by sparite cements. We suggest that fluid flow through this impermeable carbonate formation is directly related to fracturing, as indicated by the veins related to the Late Cretaceous compressional event.

Our data suggest that the groundwater flow through the Açu aquifer that was present in the Late Cretaceous is similar to the groundwater flow observed in the present-day Açu aquifer (Frischkorn and Santiago, 2000). Therefore, the assumption can be made that the groundwater flow through the Açu Formation has remained unchanged from Late Cretaceous times on, and that the fractures of Miocene age formed under similar hydrogeological conditions as the fractures of Late Cretaceous age. Nevertheless, all the Miocene fracture are uncemented and lack signs of having accommodated fluid flow. Rather than fracture closure through vein cementation, closure of the Miocene fractures probably resulted from decreasing differential stresses towards the end of the tectonic event.

The reason for the absence of fluid flow in the Miocene is most likely related to the intensity of fracturing. The density of the Cretaceous fracture network is clearly higher in the field compared to the density of the fracture network related to the Miocene compression. Whereas Late Cretaceous fractures are abundant in all outcrops, Miocene fractures were only encountered in outcrops Ap2, Ap6, DS3 and in the outcrops NW of Mossoró. Therefore, the Miocene compression probably did not manage to fracture the Jandaíra formation to such extents that an interconnected network of fractures that reached down to the Açu Formation was created. Consequently, intense fluid circulation and vein cementation was absent in the Jandaíra Formation during the Miocene.

7. Conclusions

The Turonian to Campanian Jandaíra carbonate platform demonstrates a close relation between fracturing and fluid flow. The marine regression that marked the end of deposition of marine carbonate rocks brought the Jandaíra Formation in a subaerial position. As a consequence, meteoric waters flushed out marine

connate waters, provoking diagenetic alteration of the micrites and full cementation the marine Jandaíra limestones. NNE-SSW directed tectonic compression in the Late Cretaceous to Early Tertiary created an interconnected network of fractures. This caused the previously tight Jandaíra Formation to become permeable and accommodate fluid flow. The permeability increase induced upwelling of groundwater from the underlying Açu aquifer, which was charged by rainwater in an outcropping band towards the southwest. This fluid circulation caused vein cementation at depths of 400–900 m during early burial of the Jandaíra Formation in the Late Cretaceous. At the termination of this tectonic event, the vein cementation allowed the Jandaíra Formation to regain its impermeable characteristics. In Miocene times, renewed compression was insufficiently intense to create an extensive interconnected network of open fractures capable of establishing fluid flow from the Açu sandstones into the Jandaíra Formation. In short, the Jandaíra Formation has experienced important permeability variations through time. As a result, it functioned alternatively as a sealing or a permeable unit.

Acknowledgements

This study is part of the POROCARSTE project, which involves close collaboration of the VU University Amsterdam, the Delft University of Technology and the Federal University of Rio Grande do Norte (UFRN). The POROCARSTE project is financially supported and made possible by Petrobras and the Brazilian National Petroleum Agency (ANP). The support of Suzan Verdegaal in the stable isotope laboratory was indispensable for effective and successful isotope analyses. Bauk Lacet is acknowledged for manufacturing the thin sections. Finally, the contribution of Frida Hameka, Mariska van Eijk, Brigit Oskam, Eva van der Voet and Annelieke Vis in making this into a successful project was highly appreciated.

References

Almeida, Y.B., Julià, J., Frassetto, A., 2015. Crustal architecture of the Borborema Province, NE Brazil, from receiver function CCP stacks: implications for Mesozoic stretching and Cenozoic uplift. Tectonophysics 649, 68–80.
Araripe, P.T., Feijó, F.J., 1994. Bacia potiguar. Bol. Geociências Petrobras 8, 127–141.
Assumpção, M., 1992. The regional intraplate stress field in south America. J. Geophys. Res. 97, 11889–11903.
Barbosa, J.A., Souza, E.M., Lima Filho, M.F., Neumann, V.H., 2003. A estratigrafia da Bacia Paraíba: uma reconsideração. Estud. Geol. 13, 89–108.
Barker, S.L.L., Cox, S.F., Eggins, S.M., Gagan, M.K., 2006. Microchemical evidence for episodic growth of antitaxial veins during fracture-controlled fluid flow. Earth Planet. Sci. Lett. 250, 331–344.
Bertotti, G.V., De Graaf, S., Bisdom, K., Oskam, B., Vonhof, H.B., Reijmer, J.J.G., Bezerra, F.H.R., Cazarin, C.L., 2016. Fracturing and flow during post-rift subsidence in carbonate rocks of the Jandaíra Formation, Potiguar Basin, NE Brazil. Basin Res.
Bezerra, F.H.R., Vita-Finzi, C., 2000. How active is a passive margin? Paleoseismicity in northeastern Brazil. Geology 28, 591–594.
Brito Neves, B.B., Fuck, R.A., Cordani, U.G., Thomas, A., 1984. Influence of basement structures on the evolution of the major sedimentary basins of Brazil: a case of tectonic heritage. J. Geodyn. 1, 495–510.
Buhmann, D., Dreybrodt, W., 1985. The kinetics of calcite dissolution and precipitation in geologically relevant situation of karst areas. 2. Closed system. Chem. Geol. 53, 109–124.
De Castro, D.L., Bezerra, F.H.R., Sousa, M.O.L., Fuck, R.A., 2012. Influence of Neoproterozoic tectonic fabric on the origin of the Potiguar Basin, northeastern Brazil and its links with West Africa based on gravity and magnetic data. J. Geodyn. 54, 29–42.
Chang, H.K., Kowsmann, R.O., Figueiredo, A.M.F., Bender, A.A., 1992. Tectonics and stratigraphy of the east Brazil rift system: an overview. Tectonophysics 213, 97–138.
Craig, H., 1961. Isotopic variations in meteoric waters. Science 133, 1702–1703.
Da Nóbrega, M.A., Sá, J.M., Bezerra, F.H.R., Hadler Neto, J.C., Iunes, P.J., Guedes, S., Tello Saenz, C.A., Hackspacher, P.C., Lima-Filhoa, F.P., 2005. The use of apatite fission track thermochronology to constrain fault movements and sedimentary basin evolution in northeastern Brazil. Radiat. Meas. 39, 627–633.
Dansgaard, W., 1964. Stable isotopes in precipitation. Tellus A 16, 436–468.
De Castro, D.L., 2011. Gravity and magnetic joint modeling of the Potiguar Rift Basin (NE Brazil): basement control during Neocomian extension and deformation. J. S. Am. Earth Sci. 31, 186–198.
Delicio, M.P., Coimbra, J.C., Carreño, A.L., 2000. Cretaceous marine ostracoda from the Potiguar Basin, Northeastern Brazil. Neues Jahrb. für Geol. Palaöntologie, Abh. 215, 321–345.
Dietrich, D., McKenzie, J.A., Song, H., 1983. Origin of calcite in syntectonic veins as determined from carbon-isotope ratios. Geology 11, 547–551.
Everett, C.E., Wilkinson, J.J., Rye, D.M., 1999. Fracture-controlled fluid flow in the Lower Palaeozoic basement rocks of Ireland: implications for the genesis of Irish-type Zn-Pb deposits. In: McCaffrey, K.J.W., Lonergan, L., Wilkinson, J.J. (Eds.), Fractures, Fluid Flow and Mineralization. Geological Society, vol. 155. Special Publications, London, pp. 247–276.
Fernandes, A.L., Medeiros, W.E., Bezerra, F.H.R., Oliveira, J.G., Cazarin, C.L., 2015. GPR investigation of karst guided by comparison with outcrop and unmanned aerial vehicle imagery. J. Appl. Geohpysics 112, 268–278.
Ferreira, J.M., Oliveira, R.T., Takeya, M.K., Assumpção, M., 1998. Superposition of local and regional stresses in northeast Brazil: evidence from focal mechanisms around the Potiguar basin. Geophys. J. Int. 134, 341–355.
Frischkorn, H., Santiago, M.M.F., 2000. Paleoáguas Em Bacias Sedimentares Do Nordeste, 1st Joint World Congress on Groundwater. 10 p.
Frischkorn, H., Santiago, M.F., Torquato, J.R., 1988. Dados Isotópicos e Hidroquímicos da Porçao Oriental da Bacia Potiguar. Congr. Bras. Aguas Subterrâneas 5, 144–153.
Hancock, P.L., 1985. Brittle microtectonics: principles and practice. J. Struct. Geol. 7, 437–457.
Harman, R.R., Gallagher, K., Brown, R., Raza, A., Bizzi, L., 1998. Accelerated denudation and tectonic/geomorphic reactivation of the cratons of northeastern Brazil during the Late Cretaceous. J. Geophys. Res. 103, 27091–27105.
Hoefs, J., 1973. Stable Isotope Geochemistry. Springer, New York, N.Y.:, 142 p.
Hudson, J.D., 1977. Stable isotopes and limestone lithification. Geol. Soc. Lond. 133, 637–660.
Huntoon, P.W., Lundy, D.A., 1979. Fracture-controlled ground-water circulation and well siting in the vicinity of Laramie, Wyoming. Ground Water 17, 463–469.
Japsen, P., Bonow, J.M., Green, P.F., Cobbold, P.R., Chiossi, D., Lilletveit, R., Magnavita, L.P., Pedreira, A., 2012. Episodic burial and exhumation in NE Brazil after opening of the South Atlantic. GSA Bull. 124, 800–816.
Kim, S., O'Neil, J., 1997. Equilibrium and nonequilibrium oxygen isotope effects in synthetic carbonates. Geochimica Cosmochimica Acta 61, 3461–3475.
Lattman, L.H., Parizek, R.R., 1964. Relationship between fracture traces and the occurrence of ground water in carbonate rocks. J. Hydrol. 2, 73–91.
Lima, C.C., Nascimento, E., Assumpção, M., 1997. Stress orientation in Brazilian sedimentary basins from breakout analysis—implications for force models in the South American Plate. Geophys. J. Int. 130, 112–124.
Luz, R.M.N., Julià, J., Do Nascimento, A.F., 2015. Bulk crustal properties of the Borborema Province, NE Brazil, from P-wave receiver functions: implications for models of intraplate Cenozoic uplift. Tectonophysics 644–645, 81–91.
Maia, R.P., Bezerra, F.H.R., 2015. Potiguar Basin: Diversity of landscapes in the Brazilian equatorial margin. In: Vieira, B.C., et al. (Eds.), Landscapes and Landforms of Brazil, pp. 147–156.
Maraschin, A.J., Mizusaki, A.M.P., De Ros, L.F., 2004. Near-surface K-Feldspar precipitation in cretaceous sandstones from the Potiguar Basin, Northeastern Brazil. J. Geol. 12, 317–334.
Matos, R.M., 1992. The Northeast Brazilian rift system. Tectonics 11, 766–791.
Matos, R.M., 1999. History of the Northeast Brazilian rift sytem: kinematic implications for the Break-up between Brazil and West Africa. Geol. Soc. Lond. Spec. Publ. 153, 55–73.
Matos, R.M., 2000. Tectonic evolution of the equatorial South Atlantic. In: Mohriak, W.U., Talwani, M. (Eds.), Atlantic rift and Continental Margins, vol. 155. AGU Geophysical Monograph, pp. 331–354.
McCaig, A.M., Wickham, S.M., Taylor, H.P., 1990. Deep fluid circulation in alpine shear zones, Pyrenees, France: field and oxygen isotope studies. Contributions Mineralogy Petrology 106, 41–60.
McManus, K.M., Hanor, J.S., 1988. Calcite and iron sulfide cementation of Miocene sediments flanking the West Hackberry salt dome, Southwest Louisiana, U.S.A. Chem. Geol. 74, 99–112.
Mizusaki, A.M.P., Thomaz-Filho, A., Milani, E.J., Césero, P., 2002. Mesozoic and Cenozoic igneous activity and its tectonic control in northeastern Brazil. J. S. Am. Earth Sci. 15, 183–198.
Morad, S., Al-Aasm, I.S., Sirat, M., Sattar, M.M., 2010. Vein calcite in cretaceous carbonate reservoirs of Abu Dhabi: record of origin of fluids and diagenetic conditions. J. Geochem. Explor. 106, 156–170.
Morais Neto, J.M., Hegarty, K.A., Karner, G.D., Alkmim, F.F., 2009. Timing and mechanisms for the generation and modification of the anomalous topography of the Borborema Province, northeastern Brazil. Mar. Petroleum Geol. 26, 1070–1086.
O'Neil, J.R., Clayton, R.N., Mayeda, T.K., 1969. Oxygen isotope fractionation in divalent metal carbonates. J. Chem. Phys. 51, 5547–5558.
Ojeda, H.A., 1982. Structural framework, stratigraphy, and evolution of Brazilian marginal basins. AAPG Bull. 66, 732–749.
Oliveira, R.G., Medeiros, W.E., 2012. Evidences of buried loads in the base of the crust of the Borborema Province (NE Brazil) from Bouguer admittance estimates. J. S. Am. Earth Sci. 37, 60–76.
Pascal, C., Cloetingh, S.A.P.L., 2009. Gravitational potential stresses and stress field of passive continental margins: insights from the south-Norway shelf. Earth Planet. Sci. Lett. 277, 464, 373.
Peulvast, J.P., Sales, V.C., Bétard, F., Gunnell, Y., 2008. Low post-Cenomanian

denudation depths across the Brazilian Northeast: implications for long-term landscape evolution at a transform continental margin. Glob. Planet. Change 62, 39–60.
Prikryl, J.D., Posey, H.H., Kyle, J.R., 1988. A petrographic and geochemical model for the origin of calcite cap rock at Damon Mound salt dome, Texas, U.S.A. Chem. Geol. 74, 67–97.
Ramsay, J.G., 1980. The crack-seal mechanism of rock deformation. Nature 284, 135–139.
Reddy, M.M., Plummer, L.N., Busenberg, E., 1981. Crystal growth of calcite from calcium bicarbonate solutions at constant PCO2 and 25°C: a test of a calcite dissolution model. Geochimica Cosmochimica Acta 45, 1281–1289.
Reis, A.F.C., Bezerra, F.H.R., Ferreira, J.M., Do Nascimento, A.F., Lima, C.C., 2013. Stress magnitude and orientation in the Potiguar Basin, Brazil: implications on faulting style and reactivation. J. Geophys. Res. Solid Earth 118.
Sampaio, A.V., Schaller, H., 1968. Introduçao à Estratigrafia da Bacia Potiguar. Bol. Técnico Petrobras 11, 19–44.
Santos Filho, M.A.B., Piovesan, E.K., Fauth, G., Srivastava, N.K., 2015. Paleoenvironmental interpretation through the analysis of ostracodes and carbonate microfacies: study of the Jandaíra formation, upper cretaceous, Potiguar Basin. Braz. J. Geol. 45, 23–34.
Slobodník, M., Muchez, Ph, Král, J., Keppens, E., 2006. Variscan veins: record of fluid circulation and Variscan tectonothermal events in Upper Palaeozoic limestones of the Moravian Karst, Czech Republic. Geol. Mag. 143, 491–508.
Stahl, W.J., 1979. Carbon isotopes in petroleum geochemistry. In: Hunziker, E.J. (Ed.), Lectures in Isotope Geology. Springer, New York, NY, pp. 274–283.
Suchy, V., Heijlen, W., Sykorova, I., Muchez, Ph, Dobes, P., Hladikova, J., Jackova, I., Safanda, J., Zeman, A., 2000. Geochemical study of calcite veins in the Silurian and Devonian of the Barrandian Basin (Czech Republic): evidence for widespread post-Variscan fluid flow in the central part of the Bohemian Massif. Sediment. Geol. 131, 201–219.
Tillman, J.E., Barnes, H.L., 1983. Deciphering fracturing and fluid migration histories in Northern Appalachian basin. AAPG Bull. 67, 692–705.
Turner, J.P., Green, P.F., Holford, S.P., Lawrence, S.R., 2008. Thermal history of the Rio Muni (West Africa)-NE Brazil margins during continental breakup. Earth Planet. Sci. Lett. 270, 354–367.
Vonhof, H.B., Breukelen, M.R., Postma, O., Rowe, P.J., Atkinson, T.C., Kroon, D., 2006. A continuous-flow crushing device for on-line d2H analysis of fluid inclusion water in speleotherms. Rapid Commun. Mass Spectrom. 20 (20), 2553–2558.
Vonhof, H.B., Atkinson, T.C., Van Breukelen, M.R., Postma, O., 2007. Fluid inclusion hydrogen and oxygen isotope analyses using the “Amsterdam Device”: a progress report. Geophys. Res. Abstr. 9, 05702.
Zheng, Y.F., Hoefs, J., 1993. Stable isotope geochemistry of hydrothermal mineralizations in the Harz Mountains: I. Carbon and oxygen isotopes of carbonates and implications for the origin of hydrothermal fluids. Monogr. Ser. Mineral Deposits 30, 169–187.